

Understanding the Decreased Segmental Dynamics of Supported Thin Polymer Films Reported by Incoherent Neutron Scattering

Changhuai Ye,[†] Clinton G. Wiener,[†] Madhusudan Tyagi,^{‡,||} David Uhrig,[⊥] Sara V. Orski,[§] Christopher L. Soles,[§] Bryan D. Vogt,[†] and David S. Simmons^{*,†}

[†]Department of Polymer Engineering, University of Akron, Akron, Ohio 44325, United States

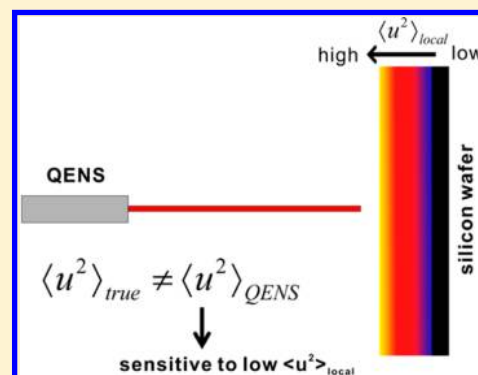
[‡]Center for Neutron Research and [§]Materials Science and Engineering Division, National Institute of Standards and Technology, Gaithersburg, Maryland 20899, United States

^{||}Department of Materials Science and Engineering, University of Maryland, College Park, Maryland 20742, United States

[⊥]Center for Nanophase Materials Science, Oak Ridge National Laboratory, Oak Ridge, Tennessee 37831, United States

S Supporting Information

ABSTRACT: Incoherent neutron scattering (INS) has commonly reported a suppression of segmental dynamics for supported thin polymer films as thickness is decreased, which is counter to expectations based on other measurement techniques such as ellipsometry and fluorescence. Here INS is utilized to measure the dynamics of thin films of comb polystyrene (PS) from 50 to 525 K. There is a significant suppression in dynamics as determined from the ~ 5 ns Debye–Waller factor, $\langle u^2 \rangle$, as measured via INS for films as thick as 213 nm, while there is no change in the glass transition temperature (T_g) as determined by ellipsometry for films as thin as 20 nm. This poor correlation between T_g from ellipsometry and dynamics as measured by $\langle u^2 \rangle$ is attributed to contamination of nanosecond $\langle u^2 \rangle$ by incipient relaxation processes, differences in sensitivity to the postulated dynamically dead layer near the substrate due to the relative weighting of the distribution of dynamics between the two techniques, differences in the time scales probed, and possible decoupling between fast and slow dynamics under nanoconfinement. These results suggest that branching of PS significantly increases the interactions with the substrate to suppress the dynamics. Both technique-specific sensitivity to time scales and its weighing of the average over the gradient in dynamic properties present at the interfaces are important to consider when qualitatively different phenomena are inferred from different measurements.



INTRODUCTION

Nanoconfinement in nanopores,¹ thin films,^{2,3} or internal nanodomains^{4–6} can dramatically influence the glass formation behavior and associated dynamic⁷ and mechanical properties⁸ of polymers and other glass-forming materials. Significant effort has been applied to studying nanoconfinement effects in polymer films due to their ease of fabrication and broad applicability in coatings,⁹ membranes,¹⁰ and microlithography.¹¹ However, the observed effect of nanoconfinement appears to depend strongly on the physical property under consideration. For example, polystyrene (PS) supported on silicon is commonly observed to exhibit a large suppression in T_g as measured by ellipsometry^{12,13} and fluorescence,¹⁴ yet incoherent neutron scattering (INS) measurements of high frequency dynamics have suggested a suppression in mobility and corresponding enhancement in T_g .¹⁵ Given that PS is commonly employed as a model system in studies of nanoconfinement,^{16–18} this apparent discord presents a considerable challenge to the developing understanding of nanoconfinement effects on the glass transition. Here we address the observation of apparently opposing trends in high

frequency dynamics, as measured by neutron scattering, and low frequency dynamics, presumably reflected by measurements of ellipsometric T_g .

A common explanation for deviations in T_g for thin films relative to the bulk is a distribution of dynamics through the film thickness,¹⁹ ascribed to interfacial effects at the polymer–air and polymer–substrate interfaces.^{20–23} The gradients in supported films are frequently approximated by three distinct layers:²⁴ a near-surface layer with enhanced mobility and suppressed T_g ,^{18,25} a central bulk-like layer; and a substrate-adjacent layer that, depending on the strength of substrate–polymer attractions, may exhibit suppressed dynamics and elevated T_g .^{12,26} The differences in the dynamics of these domains can be quite large; polymer chains are in many cases found to adsorb irreversibly to the substrate,^{27–31} even when a reduction in T_g is observed via ellipsometry for the polymer film. Pseudothermodynamic properties can likewise vary

Received: August 28, 2014

Revised: January 7, 2015

Published: January 23, 2015

strongly through the film; neutron reflectivity of selectively deuterated PS multilayer films has revealed significant differences in thermal expansion for bulk, near-surface, and near-substrate regions.^{32,33} These measurements have shown enhanced thermal expansion near the free surface with an associated decrease in T_g , while the layer near the substrate appears to have a near zero coefficient of thermal expansion (CTE).^{32,33} The question of whether the transitions between these regions are gradual^{18,21,34–36} or abrupt remains unsettled,⁷ but these interfacial gradients can be quite long range; for example, the gradient in T_g extends up to tens of nanometers into the film.^{18,32}

These competing effects between the substrate and the free surface play an important role in determining whether T_g will increase or decrease for a given polymer–substrate system.³⁷ Furthermore, they suggest that apparent qualitative discrepancies in nanoconfinement effects observed through different measurement techniques may be a result, at least in part, of their relative sensitivities to different domains within the film. However, most thin film measurements provide only an average of the T_g (or dynamics), with the time and/or length scale sensitivities intrinsic to these measurements determining how this average is obtained. Thus, the sensitivity to these different apparent layers in the film may be strongly dependent on the measurement technique selected. For example, the temperature-dependent thickness variations quantified with ellipsometry³⁸ or reflectivity³⁹ will likely be most sensitive to the more thermally expansive “layers” (e.g., surface and bulk), and these measurements tend to find that T_g decreases with decreasing film thickness as the fraction of surface layer increases.

To better understand how nanoconfinement impacts glass formation in polymer thin films, several groups have begun to systematically investigate the impact of bulk polymer properties such as tacticity in poly(methyl methacrylate),⁴⁰ the pendant groups on PS,⁴¹ or the length of alkyl side chains in methacrylates⁴² on nanoconfinement effects. No simple relationship of T_g alteration to bulk glass formation behavior, such as the size of the cooperatively rearranging regions (CRR) as determined from the Donth method⁴³ in the Adam–Gibbs⁴⁴ context, was found in these cases, but simulation work has suggested that the range of interfacial alterations in dynamics is related to the size scale of CRRs.^{34,45,46} Additionally, recent work from Torkelson and co-workers has suggested that fragility,⁴⁷ a measure of the abruptness in temperature glass formation process, is well correlated with the magnitude of T_g alterations.⁴⁸ Since the Adam–Gibbs theory of glass formation suggests that more fragile glass-formers exhibit larger scale CRRs,⁴⁴ these two observations are qualitatively consistent.

Recently, it has become clear that these thin film nanoconfinement effects are sensitive to subtle differences in interfacial interactions⁴⁰ associated with changes in polymer architecture, since adsorption interactions^{49,50} and interfacial tension^{51,52} are modified by chain branching and tacticity. For example, Glynos et al.⁵³ illustrated that the thickness dependence of T_g with star PS architectures is dependent on the number of branched chains, f , and the molecular mass, M_n , of the arm. For small f and large M_n 's on the arms in thin star PS films, the T_g depression is consistent with linear PS, but as f increases and/or M_n decreases, an inversion occurs with T_g increasing as the film thickness decreases.⁵³ This increase in T_g has been attributed to stronger adsorption of the PS at the substrate with increasing number of arms on the star.⁵³ In a similar vein, Nealey and co-workers suggested that the T_g of

supported polymer thin films increases linearly with the strength of polymer–substrate adhesion.¹² The aging rate for star PS is also dependent on f and M_n of the arms.^{54,55} These results suggest that chain architecture effects might also display different sensitivities to thin film nanoconfinement when probed with the different measurement techniques and thereby provide further insight into the roles of the different interfaces and help to rationalize the apparent “discrepancies” in the literature.

As T_g measurements are generally interpreted in terms of dynamics,⁵⁶ direct measures of dynamics in the thin polymer films can prove quite useful. Unlike dielectric spectroscopy, no modifications to the substrate for electrical connections are required with inelastic neutron scattering (INS), so these neutron techniques should provide ideal measurement techniques for direct comparison between standard measurements, such as ellipsometry or fluorescence intensity, and direct dynamic measurements. However, prior INS measurements of PS films supported on silicon substrates indicate a decrease in high frequency mobility and suggest a corresponding enhancement in apparent T_g for thin PS films,⁵⁷ which is counter to most ellipsometry^{18,38,58,59} and fluorescence intensity^{14,38} measurements. In the past, seemingly contradictory trends in apparent T_g have been rationalized in terms of the differing sensitivity of a fixed-time-window experiment to different relaxation processes.⁵⁷ A prior comparison of fluorescence intensity and ellipsometry measurements illustrated the greater sensitivity of fluorescence to the free surface, leading to a greater reduction in T_g reported by fluorescence intensity measurements.³⁸ This implies that INS may be more sensitive to the slow dynamics associated with the substrate interface than ellipsometry or fluorescence.

In order to gain further insight into the dependence of the measurement technique on the reported nanoconfinement effect, here we employ INS to study dynamics of a silicon-supported comb PS that has a thickness-invariant ellipsometric T_g down to approximately 10 nm (see Figure S3B in Supporting Information).⁶⁰ Since INS measurements are primarily sensitive to hydrogen atom density,^{60,61} this approach enables comparison with prior results for different architectures (linear, star,^{54,55} hyperbranched,⁶¹ comb, and centipede⁶⁰) of PS by retaining a similar polymer chemistry. Unlike ellipsometric results, INS measurements used here suggest an enhancement of T_g and concurrent suppression in nanosecond-time scale dynamics, at all temperatures, as thickness is reduced. This difference between INS and ellipsometry measurements is consistent with prior reports for linear PS.⁵⁷ Implicit in the impression of a contradiction between these measurements are the assumptions that T_g can be inferred from nanosecond time scale measurements of the Debye–Waller factor $\langle u^2 \rangle$ and that $\langle u^2 \rangle$ should track in some universal way with the structural relaxation time of the polymer. Here we argue that neither of these assumptions is valid and that these two measurements may therefore be entirely consistent. This outcome is consistent with a growing body of evidence that suggests commonly held relationships between T_g and other physical properties, such as mechanical response^{62–84} that are valid for bulk polymers may fail in nanoconfined materials.

EXPERIMENTAL SECTION

Materials. Comb polystyrene (PS) was synthesized as reported previously.⁶⁰ The mass average molecular mass, M_w , for comb PS was determined to be 734 kg/mol with a dispersity, D_M , of 1.06 from size

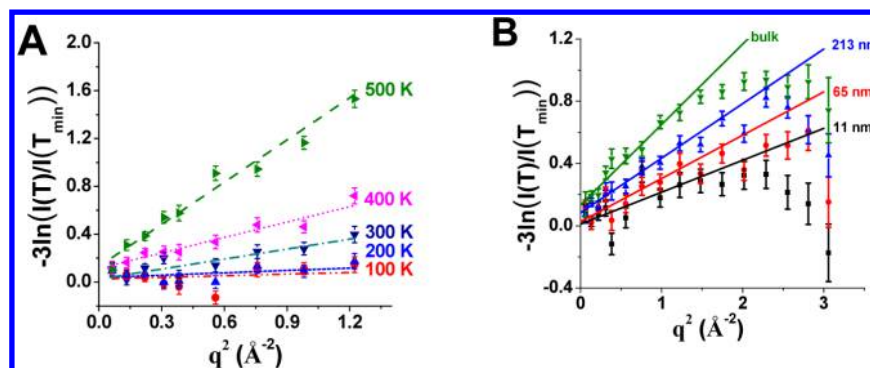


Figure 1. (A) Determination of $\langle u^2 \rangle$ from linear fit of $-3 \ln(I(T)/I(T_{\min}))$ versus q^2 for $q^2 < 1.22 \text{ \AA}^{-2}$ for 65 nm comb PS thin film at different temperatures. (B) The scattering deviates from linearity at higher q , and the deviation appears to be dependent on film thickness as shown for data at 300 K. Error bars throughout the text represent one standard deviation.

exclusion chromatography (SEC) equipped with refractive index and light scattering detection. From SEC, the average number of branches per chain was estimated to be 6.3 with M_w of approximately 60 kg/mol for each arm associated with comb branch. DSC measurements of T_g and the heat capacity, following the method described by Simon and co-workers,⁶⁵ suggest that there is no difference in the fragility, m , of the PS based on architecture between linear and comb for bulk samples ($m = 144 \pm 7.5$ and 150.1 ± 6.6). The fragility of the polymer has been reported to be a key aspect for understanding nanoconfinement effects,⁴⁸ but there are exceptions such as polymethacrylates.

Sample Preparation. To prepare bulk sample, 0.38 g of comb PS was sandwiched by 4 cm \times 9.5 cm aluminum foil layers. The sandwiched sample was subsequently molded to approximately 0.1 mm thick by compression at 185 °C. 76.2 mm diameter silicon wafers (Silicon Inc.) with a thickness of 0.2 mm were used as the substrates for the thin films. Prior to spin-coating the comb PS films, the silicon wafers were cleaned using UV-ozone cleaner (Model No. 42, Jelight Co., Inc.) for 5 min. Comb PS thin films were spun-cast from toluene at 3000 rpm. The thin films were then annealed at 120 °C under vacuum for 2 h to remove the residual solvent.

X-ray Reflectivity. The thicknesses of the comb PS thin films were measured using X-ray reflectivity prior to performing the neutron scattering experiments. The reflectivity was collected in a $\theta/2\theta$ geometry using Cu K α radiation focused by a bent crystal mirror into a 4-bounce Ge (220) crystal monochromator. The reflected beam was further collimated through a 3-bounce channel cut Ge (220) crystal prior to detection. The thickness of the films was fit by recursive modeling using REFLPAK software suite.⁶⁶

Neutron Scattering. Incoherent neutron scattering (INS) measurements were performed on the NG-2 high flux backscattering spectrometer (HFBS) at NIST Center for Neutron Research (NCNR). All measurements utilized 6.271 Å wavelength (λ) cold neutrons with energy of 2.08 meV. All 16 detectors, 1–3 low angle detectors and 4–16 high angle detectors, were used to realize an effective q range of 0.25–1.75 Å⁻¹, where $q = 4\pi/\lambda \sin(\theta)$ and θ is scattering angle. The instrument resolution is approximately 0.85 μ eV with an associated time scale of 200 MHz for the dynamic window.

The supported films were placed into cylindrical aluminum cans (29 mm diameter and 50 mm high) for the HFBS measurements. To fill the sample cell, the silicon wafers coated with the comb PS thin films were cleaved into rectangular pieces. Each sample cell was filled with approximately 16 pieces of the cleaved 75 mm wafers, resulting in approximately 0.8–15 mg of the active polymer film being probed in the HFBS experiments. Each sample was loaded under helium and sealed with a lead gasket to ensure excellent heat transfer among different pieces. For the backscattering measurements, each sample was first cooled to 50 K and then heated to 525 K at the rate of 0.2 K/min (thin films) or 1 K/min (bulk sample), and each data point was averaged over 600 s in the films and 60 s in the bulk. The incident beam was approximately orthogonal to the plane of the supported thin film. The data were analyzed by DAVE software.⁶⁷

RESULTS AND DISCUSSION

As the scattering intensity is proportional to the number of scatterers (and thus to film thickness), the elastic intensity was normalized to the intensity at the lowest temperature ($T = 50$ K) following the same protocol as reported previously⁶⁸ in order to enable comparison between different thicknesses of films. In order to quantify the mobility of the polymer segments (apparent Debye–Waller factor, DWF), the mean-squared-displacement, $\langle u^2 \rangle$, is determined from the elastic intensity according to the Debye–Waller approximation as

$$I_{\text{elastic}} = I_0 \exp\left(-\frac{q^2}{3} \langle u^2 \rangle\right) \quad (1)$$

where I_0 is purely elastic intensity from the sample. I_0 is usually measured at very low temperatures, which is in our case is 50 K. This model assumes that the motions responsible for the decrease in the elastic scattering intensities can be modeled as simple harmonic (Gaussian) with $\langle u^2 \rangle$ representing the average mean-square-displacement of the hydrogen-containing moieties moving faster than approximately 200 MHz (resolution of the spectrometer).

To calculate $\langle u^2 \rangle$, the HFBS data is plotted as $\ln(I_{\text{elastic}})$ vs q^2 , as shown in Figure 1, with the linear slope directly yielding $\langle u^2 \rangle$. This is shown for a variety of temperatures in Figure 1A for the 65 nm thick comb PS film. However, significant nonlinearity is clearly observed for $q^2 > 1.22 \text{ \AA}^{-2}$ as shown in Figure 1B. Similar deviations have been previously observed in PMMA films as well.⁶⁹ By combining the Gaussian component with a non-Gaussian component for the displacement, an improved fit can be obtained, but this fitting introduces several additional parameters that combined with the uncertainty in the data due to the small scattering volume associated with the thin films leads to minimal additional physical understanding. As such, only the linear, Gaussian contribution at $q^2 < 1.22 \text{ \AA}^{-2}$ is fit to determine $\langle u^2 \rangle$ as illustrated in Figure 1A.

Figure 2 illustrates the temperature dependence of $\langle u^2 \rangle$ determined via eq 1 for the comb PS films. These data contain two features that have previously been interpreted⁵⁷ as indicating suppression in mobility and an increase in T_g with reducing film thickness. First, the relatively abrupt change in slope of $\langle u^2 \rangle$ as a function of temperature, which is commonly associated with T_g ,^{57,69} shifts to higher temperature with decreasing film thickness. Second, $\langle u^2 \rangle$ is reduced with decreasing film thickness, suggesting a reduction in nano-second-time scale mobility. These observations are surprising in

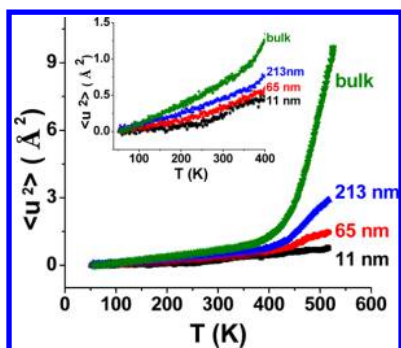


Figure 2. Change of $\langle u^2 \rangle$ with temperature for bulk comb PS and its thin films. The inset more clearly illustrates the difference in low temperature dynamics associated with the β relaxation.

several respects. First, the apparent enhancement in T_g based on the bend in $\langle u^2 \rangle$ is inconsistent with the bulk-like T_g observed in ellipsometric measurements of this system. Second, whereas $\langle u^2 \rangle$ is suppressed compared to the bulk even for the 213 nm thick comb PS film, nanoconfinement effects on the physical properties of thin films are typically (with limited exceptions⁴¹) not observed for films thicker than 100 nm, with observable effects typically beginning closer to 40 nm. Prior backscattering measurements with linear PS illustrated a slightly reduced mobility for 100 nm thin films,⁵⁷ but significantly weaker than observed here for the comb PS. This suggests a stronger nanoconfinement effect for comb PS than linear PS, in direct contrast to prior measurements of T_g and modulus in these materials, where a very limited nanoconfinement effect was observed for the comb PS.⁶⁰ Finally, the reduced mobility reflected in $\langle u^2 \rangle$ is again in direct apparent contradiction to the observed negligible alteration in T_g of this system for thicknesses greater than 11 nm as determined by ellipsometry. This begs the question: How can we understand these apparent discrepancies?

In order to understand these observations, we now address the following three questions. First, what is the meaning of the “kink” in $\langle u^2 \rangle$? Is it reasonable to identify the position of this “kink” with T_g for the purpose of quantifying trends under nanoconfinement? Second, what is the relationship between the measured $\langle u^2 \rangle$ and the structural relaxation time (and, correspondingly, T_g)? Should we expect them to trend in the same direction in thin films? Third, what is the relationship

between the spring constant (stiffness) determined from $\langle u^2 \rangle$ and film moduli as measured by wrinkling experiments?

We begin by considering the observation of an apparent increase in T_g with reduced film thickness as measured by the change in slope of the temperature dependence of $\langle u^2 \rangle$. This is similar to prior reports on T_g as determined by INS measurements of linear PS thin films, which exhibit an inverse relationship with film thickness,⁵⁷ in apparent contradiction to the nanoconfinement-induced decrease in T_g generally observed using other techniques for linear PS films,^{18,25,59,70,71} and the absence of T_g -nanoconfinement effects via ellipsometry for comb PS.⁶⁰ It is now well-established that, in general, the validity of the position of the bend in $\langle u^2 \rangle$ measurements at the nanosecond time scales as a quantitative measure of T_g is questionable due to contamination by incipient α -relaxation near and above T_g at time scales appreciably longer than 1 ps.⁷² This bend has nevertheless been used to identify trends in T_g , presumably under the assumption that qualitative trends in apparent T_g are insensitive to contamination by α -relaxation.

Although the above view may hold in the bulk, we suggest that it is highly problematic in thin films. Specifically, if we recast the problem in terms of the intermediate scattering function (the time-Fourier transform of the scattering function), then the amount of contamination of nanosecond $\langle u^2 \rangle$ by the α -relaxation process is described by the Kohlrausch–Williams–Watts (KWW) stretched exponential form that commonly characterizes the α -relaxation process in glasses. Combining this relaxation form with the Gaussian approximation (comparable to the Debye–Waller approximation) to obtain an equation for the Debye–Waller factor yields (see Supporting Information for derivation) the equation

$$\langle u^2(t) \rangle = \langle u^2 \rangle_0 + \frac{6}{q^2} \left(\frac{t}{\tau} \right)^{\beta_{\text{KWW}}} \quad (2)$$

where β_{KWW} is the stretching exponent, τ is the α -relaxation time, $\langle u^2 \rangle_0$ is the value of the Debye–Waller factor on a picoseconds time scale, and $\langle u^2(t) \rangle$ is its value at some later time. Thus, for measurements at frequencies corresponding to time scales shorter than the α -relaxation frequency but longer than 1 ps, the amount of contamination depends on τ and β_{KWW} for the α -relaxation process. Specifically, for a given frequency measurement, lower τ or β_{KWW} will yield a higher degree of contamination.

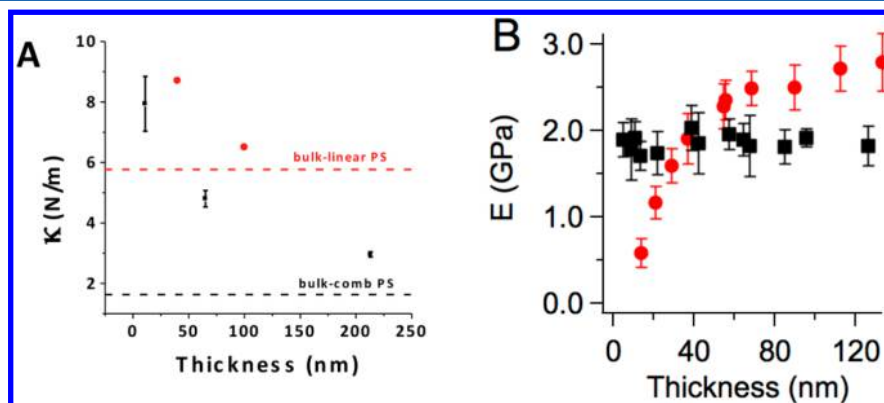


Figure 3. (A) Vibrational spring constants, κ , for bulk and thin film PS as a function of film thickness for linear⁷⁸ (●) and comb (■) PS. κ generally scales directly with elastic modulus, but (B) the modulus as determined by wrinkling⁶⁰ does not follow this trend for either of these polymers in thin films.

Equation 2 indicates that trends between systems in the T_g inferred from nanosecond $\langle u^2 \rangle$ can be viewed as qualitatively correct provided that β_{KWW} remains roughly constant, since τ at T_g is an approximate constant. This condition is likely satisfied in many bulk systems. However, evidence suggests β_{KWW} can be substantially altered under nanoconfinement, with β_{KWW} increasing near the surface⁷³ and being suppressed for the film-average relaxation.⁷ Since reducing (increasing) β_{KWW} will tend to enhance (suppress) apparent $\langle u^2 \rangle$ at the same temperature relative to T_g , the “bend” in nanosecond time scale $\langle u^2 \rangle$ vs temperature cannot be employed as a reliable indicator of trends in T_g in thin films in the absence of knowledge of β_{KWW} .

While this explanation excludes the “kink” in nanosecond time scale $\langle u^2 \rangle$ as a reliable measure of trends in T_g under nanoconfinement, it leaves unexplained the observation of a reduction in $\langle u^2 \rangle$ with decreasing film thickness at temperatures well below T_g since in this temperature range the α -relaxation process should not commence until well beyond the ~ 5 ns time window measured by INS. Under the assumption that structural α -relaxation tracks with T_g , this suggests that $\langle u^2 \rangle$ and τ_α exhibit opposing trends under nanoconfinement. Furthermore, the reduction in $\langle u^2 \rangle$ is expected, based on a Maxwell model, to reflect an enhancement in the local elastic properties of the glass;^{74,75} well below T_g , $\langle u^2 \rangle$ is inversely proportional to a local spring constant, κ , for harmonic vibration of segments within a cage of their neighbors:⁷⁶ $\kappa = 3k_B T / \langle u^2 \rangle$ where k_B is the Boltzmann constant and assuming harmonic confinement in the glass as suggested by Hall and Wolynes.⁷⁶ κ is specifically expected to scale roughly with the high frequency shear modulus.⁷⁷ The suppression in κ observed in Figure 3 with reducing film thickness is therefore surprising given that the elastic modulus of this system as measured by surface wrinkling is invariant.⁶⁰ Again, this is similar to the situation for linear PS, for which κ has been observed to grow with decreasing film thickness⁷⁸ despite a concurrent decrease in modulus as measured by surface wrinkling.⁷⁹ Why, then, do these measurements indicate a pronounced reduction in mobility and enhancement in modulus, while measurements of T_g by ellipsometry⁶⁰ and modulus by wrinkling suggest that mobility and modulus are not substantially altered for the comb PS? Equivalently, why do prior measurements in linear PS suggest a reduction in mobility based on $\langle u^2 \rangle$ measurements,⁷⁸ but an enhancement in mobility based upon ellipsometric measurements^{13,16,38} of T_g ?

One potential explanation may relate to the manner in which ellipsometric and INS measurements average over local mobility gradients within the film. As discussed in a recent paper by Forrest and Dalnoki-Veress, ellipsometric measurements reflect a thickness-averaged film T_g .⁸⁰ Similarly, INS measures the mobility of polymer thin films based on a mean $\langle u^2 \rangle$ that reflects some weighted average of the mobility of the film. Since supported films are expected to include interfacial and surface layers of suppressed and enhanced mobility, respectively, any difference in the weight given to these domains by these two methods can be expected to allow for apparently incongruous trends in T_g and mobility determined via the two methods. We can understand this weighting effect in the case of INS as follows.

First, it is well-established that $\langle u^2 \rangle$ determined by INS tends to be weighted toward the lowest frequency processes present within the time window.⁸¹ This fact indicates that any contamination by relaxation processes beyond 1 ps can be

expected to dominate the measured $\langle u^2 \rangle$. Although contamination by α -relaxation is not an issue well below T_g , previous studies have shown that additional, local, high frequency relaxation processes commonly take place in the 1 ps–10 ns window even in the glassy state.⁸² At all but the lowest temperatures, it is likely that these processes substantially impact the measured $\langle u^2 \rangle$. Since these processes are highly local and chemically specific, it is not possible to definitively conclude that trends in $\langle u^2 \rangle$ at this time scale have a clear relationship to α -relaxation and therefore to T_g .

At the lowest temperatures, these additional processes presumably freeze out such that the nanosecond $\langle u^2 \rangle$ reflects the true picosecond Debye–Waller factor. Ideally, in this temperature range the value of $\langle u^2 \rangle$ probed by INS would reflect the true number-average $\langle u^2 \rangle$. However, we now show that this is not the case, as follows. Assuming that both density and $\langle u^2 \rangle$ vary as a function of position within the film, this is given by

$$\langle u^2 \rangle = \frac{1}{\langle \rho_A \rangle} \int_{-\infty}^{\infty} \rho_A(z) \langle u^2 \rangle_A(z) dz \quad (3)$$

where $\rho_A(z)$ is the areal number density (number of scatterers per area) at a position z within the film, $\langle \rho_A \rangle$ is the thickness-average areal number density, and $\langle u^2 \rangle_A(z)$ is the area-average value of $\langle u^2 \rangle$ at a position z within the film. However, as noted above, within incoherent quasi-elastic neutron scattering experiments, the DWF is obtained from the dynamic structure factor via the Debye–Waller approximation given by eq 1. $\langle u^2 \rangle$ can thus be written as an explicit average over the depth of the film as

$$\langle u^2 \rangle_{\text{INS}} = -\frac{3}{q^2} \ln \frac{1}{\langle \rho_A \rangle} \int_{-\infty}^{\infty} \rho_A(z) \langle S(q, \omega) \rangle(z) dz \quad (4)$$

where $\langle u^2 \rangle_{\text{INS}}$ is the value of the Debye–Waller factor determined from INS and $\langle S(q, \omega) \rangle(z) \equiv (I_{\text{elastic}}/I_0)_z$ is the dynamic structure factor averaged over the film area at a depth z in the film. If we employ the Debye–Waller approximation locally at each depth within the film, this becomes

$$\langle u^2 \rangle_{\text{INS}} = -\frac{3}{q^2} \ln \left[\frac{1}{\langle \rho_A \rangle} \int_{-\infty}^{\infty} \rho_A(z) \exp \left(-\frac{q^2}{3} \langle u^2 \rangle_A(z) \right) dz \right] \quad (5)$$

Neglecting variations in density over the thickness of the film, eqs 3 and 5 can be rewritten as

$$\langle u^2 \rangle = \frac{1}{h} \int_0^h \langle u^2 \rangle_A(z) dz \quad (6)$$

where h is the thickness of the film and

$$\langle u^2 \rangle_{\text{INS}} = -\frac{3}{q^2} \ln \left[\frac{1}{h} \int_0^h \exp \left(-\frac{q^2}{3} \langle u^2 \rangle_A(z) \right) dz \right] \quad (7)$$

Comparing eqs 6 and 7 indicates that while the true film average $\langle u^2 \rangle$ is a simple linearly weighted number average over the local $\langle u^2 \rangle_A(z)$, in the limit of no contamination by relaxation processes, $\langle u^2 \rangle_{\text{INS}}$ obtained from INS is an inverse-exponentially weighted average over the local $\langle u^2 \rangle$. Thus, outside of the weighing toward lower frequencies,⁸¹ $\langle u^2(t) \rangle_{\text{INS}}$ weights regions of the film with lower local $\langle u^2 \rangle$ more strongly, such that $\langle u^2(t) \rangle_{\text{INS}} \leq \langle u^2(t) \rangle$. Furthermore, a modest enhancement in density due to attractive interactions near

the substrate coupled with a modest reduction in density proximate to the interface would be expected to further augment this weighting toward the slow, substrate adjacent $\langle u^2 \rangle$. Finally, we note that eq 7 predicts that any spatial gradient in $\langle u^2 \rangle$ should lead to a greater q -dependence of the apparent $\langle u^2 \rangle$, in the form of more pronounced nonlinearity in the normalized intensity vs q^2 . Because of the large uncertainty in intensity at high q in these measurements, it is not possible to draw any conclusions regarding this prediction from the present data; however, it could provide a potential basis for obtaining information on the spatial dependence of $\langle u^2 \rangle$ in future studies.

This weighting-based enhancement of the measured $\langle u^2 \rangle_{\text{INS}}$ over the true linear average $\langle u^2 \rangle$ is likely to be especially pronounced in comb polystyrene. Specifically, prior evidence has suggested that PS, irrespective of architecture, exhibits a dynamically “dead” layer near the substrate interface.^{53,54,78,83} In the present case for the comb polymer, the dead layer for comb PS would be predicted to be significantly more stiff and/or thicker than linear PS based on the increased κ at 213 nm for the comb PS. This could be a result of the lower entropic penalty for contact with the surface⁴⁹ and increased chain contacts with surface⁵⁰ compared to linear polymer at the same molecular weight. Moreover, the residual layer after near equilibrium dewetting is more than an order of magnitude greater for 8 arm star PS (7.8 nm) than linear PS (0.3 nm).⁸⁴ If we assume that this residual layer is correlated with the “dead layer” that exhibits reduced $\langle u^2 \rangle$, the presence of a thicker dead layer in the comb polymer would be expected to not only reduce mobility, but to yield an even greater apparent mobility reduction at the lowest temperatures probed by INS due to the weighting considerations (eq 7). This biasing of the INS data to low mobility in the absence of relaxational contamination is similar (but opposite in nature) to the reported biasing of fluorescence intensity measurements to the high mobility free surface layer.³⁸

The above discussion suggests that there are several reasons to question whether the strength of the apparent suppression in high-frequency mobility probed by ~ 5 ns INS measurements reflect the true average dynamics of the system. However, we note that concurrent observations of enhanced low-frequency dynamics and suppressed high-frequency dynamics are not necessarily intrinsically contradictory. Prior evidence from experiment, computation, and theory indicate that fast and slow relaxation processes in glasses can be decoupled under certain circumstances.^{74,85} For example, antiplasticizer additives enhance the rate of α -relaxation while simultaneously suppressing the fast β relaxation and reducing the Debye–Waller factor;⁷⁵ these changes are consistent with the observations here when comparing ellipsometry and INS measurements of polystyrene. More broadly, although numerous models posit some fundamental relationship between $\langle u^2 \rangle$ and τ_w ^{76,86–88} the details of this relationship have been shown to depend on the particular system under consideration, such that it is not appropriate to assume that shifts in $\langle u^2 \rangle$ must always track shifts in τ_w .^{88,89} In essence, it is entirely possible to enhance long-time mobility while suppressing short-time vibrational mobility, and this phenomenon may account for the presently observed results.

To further investigate the biasing toward slow dynamics in the averaging of the dynamics in thin films of polymers by INS, previous reported results from the literature can be re-examined. For thin supported films, there is a general trend for a decrease in the local dynamics as measured by INS that

does not generally correlate with measures of T_g determined by other commonly utilized techniques.⁶⁹ For example, the dynamics as denoted by $\langle u^2 \rangle$ have been reported to decrease for polycarbonate⁹⁰ upon nanoconfinement in thin supported films; however, X-ray reflectivity indicates a decrease in T_g from the kink in the thermal expansion coefficient.⁹¹ A similar result is reported for supported films of linear PS with a suppression in $\langle u^2 \rangle$,⁵⁷ while a decrease in T_g from fluorescence and ellipsometry is generally reported.^{18,25,59,70,71}

Similar arguments can be made with respect to the differences in mechanical properties assessed through κ with INS and elastic modulus with surface wrinkling. For INS with the normal incident of the neutron beam to film surface, the measurement is weighed heavily toward the in-plane dynamics. Thus, κ should provide a measure of in-plane modulus of the films. Conversely, wrinkling probes the elastic modulus through the thickness of the film for selection of the wavelength.⁹² This directional sensitivity would be important if anisotropic properties develop due to the alignment of the asymmetric rattle volume⁸⁸ associated with local dynamics. Although previous INS measurements of PMMA thin films did not exhibit any anisotropy in $\langle u^2 \rangle$, insufficient evidence is available to rule this possibility out in other systems.⁶⁸ Furthermore, similar to the discussion above, the manner in which the apparent film modulus probed by these methods weights of the distribution of moduli in the material (as would be expected from the gradients⁹³ in T_g) in the films is measurement specific. It is known that the weighing of moduli from wrinkling from the simple bilayer model is highly nonlinear and depends on the spatial distribution.⁹² For INS, we have already demonstrated herein that this measurement reports an average that is weighted more heavily toward the slow dynamic regions (higher κ) in the absence of postpicosecond to nanosecond relaxation processes. Thus, differences in the reported properties for different measurements may not be unexpected as each will weigh the distributions of properties present in the thin films by the physics dictated by the technique. The nature of the averaging of properties may explain the apparent discrepancies in the thin film literature when comparing significantly different measurement techniques.

CONCLUSIONS

The dynamics of thin films of comb PS supported on silicon wafers have been elucidated using INS. Interestingly, there is a very strong thickness dependence on the dynamics with $\langle u^2 \rangle$ suppressed significantly in comparison to the bulk, even for 213 nm thick film. This behavior is counter to expectations based on the minor decrease in T_g reported by ellipsometry that occurs only for thin films (<15 nm). Here we have shown that (1) the “kink” in $\langle u^2 \rangle$ cannot be employed as an unambiguous measure of trends in T_g absent information on the stretching exponent of the α -relaxation process and (2) for reasons of both measurement weighting and the nature of the relationship between nanosecond $\langle u^2 \rangle$ and τ_w , it is unsurprising to observe inverse trends in these properties under nanoconfinement. We specifically illustrate that, beyond the known weighting toward low-frequency processes that can be expected to cause relaxational contamination to dominate at high temperatures, at low temperatures where relaxation processes are absent from the frequency window, $\langle u^2 \rangle$ as determined from INS is weighted toward regions with low $\langle u^2 \rangle$ when considering the averaging of the distribution of dynamics through the film thickness. Moreover as T_g is approached, the measured $\langle u^2 \rangle$ is

contaminated by artificial enhancement resulting from incipient relaxation when measurements are made at time scales appreciably greater than 1 ps; this leads to a strong bias toward the kink in $\langle u^2 \rangle$ with temperature shifting to larger temperatures in thin films. Thus, the T_g inferred from INS should be utilized with great caution. Consistent with these arguments, prior reports from INS generally reported an increase in T_g or only a modest suppression in T_g .^{57,68,69,91} Moreover, we note that enhanced low-frequency dynamics and suppressed high-frequency dynamics for the same system under nanoconfinement are not necessarily intrinsically contradictory since $\langle u^2 \rangle$ and τ_α do not exhibit an invariant universal relationship.^{88,89}

In summary, the interpretation of dynamics in thin films needs to consider the distribution of dynamics in the film and the relative sensitivity of the technique to this distribution and its relative weighing. These differences in sensitivity of different measurement techniques may explain some apparent discrepancies in the literature associated with glass formation in thin polymer films. Future work in simulations should consider the averaging of the properties of glass-forming polymer films investigated to provide correspondence to the experimental limitations in the sensitivity of common techniques such as ellipsometry to understand if there is significant biasing of experimental results that could impact the fundamental understanding of glass formation under nanoconfinement.

■ ASSOCIATED CONTENT

Supporting Information

Experimental details. This material is available free of charge via the Internet at <http://pubs.acs.org>.

■ AUTHOR INFORMATION

Corresponding Author

*E-mail dsimmon@uakron.edu (D.S.S.).

Notes

The authors declare no competing financial interest.

■ ACKNOWLEDGMENTS

A portion of this research was conducted at the Center for Nanophase Materials Sciences, which is sponsored at Oak Ridge National Laboratory by the Scientific User Facilities Division, Office of Basic Energy Sciences, U.S. Department of Energy. This work utilized facilities supported in part by the National Science Foundation under Agreement No. DMR-0944772. D.S.S. acknowledges support for this work by the National Science Foundation under Grant No. DMR1310433. The identification of commercial products does not imply endorsement by the National Institute of Standards and Technology nor does it imply that these are the best for the purpose.

■ REFERENCES

- (1) Jackson, C. L.; McKenna, G. B. *J. Non-Cryst. Solids* **1991**, *131*, 221–224.
- (2) Torkelson, J. M.; Priestley, R. D.; Rittigstein, P.; Mundra, M. K.; Roth, C. B. Novel effects of confinement and interfaces on the glass transition temperature and physical aging in polymer films and nanocomposites. In *Complex Systems*; Tokuyama, M., Oppenheim, I., Nishiyama, H., Eds.; 2008; Vol. 982, pp 192–195.
- (3) Ediger, M. D.; Forrest, J. A. *Macromolecules* **2014**, *47*, 471–478.
- (4) Lang, R. J.; Merling, W. L.; Simmons, D. S. *ACS Macro Lett.* **2014**, *3*, 758–762.

- (5) Liu, R. Y. F.; Bernal-Lara, T. E.; Hiltner, A.; Baer, E. *Macromolecules* **2005**, *38*, 4819–4827.
- (6) Starr, F. W.; Douglas, J. F. *Phys. Rev. Lett.* **2011**, *106*, 115702.
- (7) Paeng, K.; Swallen, S. F.; Ediger, M. D. *J. Am. Chem. Soc.* **2011**, *133*, 8444–8447.
- (8) Peng, D.; Yang, Z.; Tsui, O. K. C. *Macromolecules* **2011**, *44*, 7460–7464.
- (9) Hiller, J.; Mendelsohn, J. D.; Rubner, M. F. *Nat. Mater.* **2002**, *1*, 59–63.
- (10) Martin, C. R. *Science* **1994**, *266*, 1961–1966.
- (11) Hawker, C. J.; Russell, T. P. *MRS Bull.* **2005**, *30*, 952–966.
- (12) Fryer, D. S.; Peters, R. D.; Kim, E. J.; Tomaszewski, J. E.; de Pablo, J. J.; Nealey, P. F.; White, C. C.; Wu, W. L. *Macromolecules* **2001**, *34*, 5627–5634.
- (13) Kawana, S.; Jones, R. A. L. *Phys. Rev. E* **2001**, *63*, 021501.
- (14) Ellison, C. J.; Kim, S. D.; Hall, D. B.; Torkelson, J. M. *Eur. Phys. J. E* **2002**, *8*, 155–166.
- (15) Inoue, R.; Kanaya, T.; Nishida, K.; Tsukushi, I.; Shibata, K. *Phys. Rev. E* **2008**, *77*, 032801.
- (16) Keddie, J. L.; Jones, R. A. L.; Cory, R. A. *Europhys. Lett.* **1994**, *27*, 59–64.
- (17) Forrest, J. A.; DalnokiVeress, K.; Stevens, J. R.; Dutcher, J. R. *Phys. Rev. Lett.* **1996**, *77*, 2002–2005.
- (18) Ellison, C. J.; Torkelson, J. M. *Nat. Mater.* **2003**, *2*, 695–700.
- (19) Ediger, M. D. *Annu. Rev. Phys. Chem.* **2000**, *51*, 99–128.
- (20) Siretanu, I.; Chapel, J. P.; Drummond, C. *Macromolecules* **2012**, *45*, 1001–1005.
- (21) Kim, S.; Torkelson, J. M. *Macromolecules* **2011**, *44*, 4546–4553.
- (22) Napolitano, S.; Pilleri, A.; Rolla, P.; Wuebbenhorst, M. *ACS Nano* **2010**, *4*, 841–848.
- (23) Roth, C. B.; Torkelson, J. M. *Macromolecules* **2007**, *40*, 3328–3336.
- (24) Fukao, K.; Miyamoto, Y. *Phys. Rev. E* **2000**, *61*, 1743–1754.
- (25) Yang, Z.; Fujii, Y.; Lee, F. K.; Lam, C.-H.; Tsui, O. K. C. *Science* **2010**, *328*, 1676–1679.
- (26) Qi, D.; Fakhraai, Z.; Forrest, J. A. *Phys. Rev. Lett.* **2008**, *101*, 096101.
- (27) Napolitano, S.; Capponi, S.; Vanroy, B. *Eur. Phys. J. E* **2013**, *36*, 61.
- (28) Rotella, C.; Napolitano, S.; De Cremer, L.; Koeckelberghs, G.; Wubbenhorst, M. *Macromolecules* **2010**, *43*, 8686–8691.
- (29) Gin, P.; Jiang, N.; Liang, C.; Taniguchi, T.; Akgun, B.; Satija, S. K.; Endoh, M. K.; Koga, T. *Phys. Rev. Lett.* **2012**, *109*, 265501.
- (30) Koga, T.; Jiang, N.; Gin, P.; Endoh, M. K.; Narayanan, S.; Lurio, L. B.; Sinha, S. K. *Phys. Rev. Lett.* **2011**, *107*, 225901.
- (31) Fujii, Y.; Yang, Z.; Leach, J.; Atarashi, H.; Tanaka, K.; Tsui, O. K. C. *Macromolecules* **2009**, *42*, 7418–7422.
- (32) Inoue, R.; Kawashima, K.; Matsui, K.; Kanaya, T.; Nishida, K.; Matsuba, G.; Hino, M. *Phys. Rev. E* **2011**, *83*, 021801.
- (33) Inoue, R.; Kawashima, K.; Matsui, K.; Nakamura, M.; Nishida, K.; Kanaya, T.; Yamada, N. L. *Phys. Rev. E* **2011**, *84*, 031802.
- (34) Lang, R. J.; Simmons, D. S. *Macromolecules* **2013**, *46*, 9818–9825.
- (35) Varnik, F.; Baschnagel, J.; Binder, K. *Phys. Rev. E* **2002**, *65*, 021507.
- (36) Hanakata, P. Z.; Douglas, J. F.; Starr, F. W. *J. Chem. Phys.* **2012**, *137*, 244901.
- (37) Forrest, J. A.; DalnokiVeress, K.; Dutcher, J. R. *Phys. Rev. E* **1997**, *56*, 5705–5716.
- (38) Kim, S.; Hewlett, S. A.; Roth, C. B.; Torkelson, J. M. *Eur. Phys. J. E* **2009**, *30*, 83–92.
- (39) Tsui, O. K. C.; Russell, T. P.; Hawker, C. J. *Macromolecules* **2001**, *34*, 5535–5539.
- (40) Grohens, Y.; Hamon, L.; Reiter, G.; Soldara, A.; Holl, Y. *Eur. Phys. J. E* **2002**, *8*, 217–224.
- (41) Ellison, C. J.; Mundra, M. K.; Torkelson, J. M. *Macromolecules* **2005**, *38*, 1767–1778.
- (42) Campbell, C. G.; Vogt, B. D. *Polymer* **2007**, *48*, 7169–7175.
- (43) Donth, E. *J. Non-Cryst. Solids* **1982**, *53*, 325–330.

- (44) Adam, G.; Gibbs, J. H. *J. Chem. Phys.* **1965**, *43*, 139–146.
- (45) Hanakata, P. Z.; Douglas, J. F.; Starr, F. W. *Nat. Commun.* **2014**, *5*, 4163.
- (46) Shavit, A.; Riggelman, R. A. *J. Phys. Chem. B* **2014**, *118*, 9096–9103.
- (47) Angell, C. A. *Science* **1995**, *267*, 1924–1935.
- (48) Evans, C. M.; Deng, H.; Jager, W. F.; Torkelson, J. M. *Macromolecules* **2013**, *46*, 6091–6103.
- (49) Striolo, A.; Prausnitz, J. M. *J. Chem. Phys.* **2001**, *114*, 8565–8572.
- (50) Kosmas, M. K. *Macromolecules* **1990**, *23*, 2061–2065.
- (51) Minnikanti, V. S.; Archer, L. A. *Macromolecules* **2006**, *39*, 7718–7728.
- (52) Qian, Z.; Minnikanti, V. S.; Sauer, B. B.; Dee, G. T.; Archer, L. A. *Macromolecules* **2008**, *41*, 5007–5013.
- (53) Glynos, E.; Frieberg, B.; Oh, H.; Liu, M.; Gidley, D. W.; Green, P. F. *Phys. Rev. Lett.* **2011**, *106*, 128301.
- (54) Frieberg, B.; Glynos, E.; Green, P. F. *Phys. Rev. Lett.* **2012**, *108*, 268304.
- (55) Frieberg, B.; Glynos, E.; Sakellariou, G.; Green, P. F. *ACS Macro Lett.* **2012**, *1*, 636–640.
- (56) Forrest, J. A. *Eur. Phys. J. E* **2002**, *8*, 261–266.
- (57) Inoue, R.; Kanaya, T.; Nishida, K.; Tsukushi, I.; Telling, M. T. F.; Gabrys, B. J.; Tyagi, M.; Soles, C.; Wu, W. I. *Phys. Rev. E* **2009**, *80*, 031802.
- (58) Pye, J. E.; Rohald, K. A.; Baker, E. A.; Roth, C. B. *Macromolecules* **2010**, *43*, 8296–8303.
- (59) Sharp, J. S.; Forrest, J. A. *Phys. Rev. Lett.* **2003**, *91*, 235701.
- (60) Torres, J. M.; Stafford, C. M.; Uhrig, D.; Vogt, B. D. *J. Polym. Sci., Part B* **2012**, *50*, 370–377.
- (61) Erber, M.; Georgi, U.; Mueller, J.; Eichhorn, K. J.; Voit, B. *Eur. Polym. J.* **2010**, *46*, 2240–2246.
- (62) Boucher, V. M.; Cangialosi, D.; Yin, H.; Schoenhals, A.; Alegria, A.; Colmenero, J. *Soft Matter* **2012**, *8*, 5119–5122.
- (63) O’Connell, P. A.; McKenna, G. B. *J. Polym. Sci., Part B* **2009**, *47*, 2441–2448.
- (64) Torres, J. M.; Stafford, C. M.; Vogt, B. D. *ACS Nano* **2009**, *3*, 2677–2685.
- (65) Koh, Y. P.; Simon, S. L. *J. Polym. Sci., Part B* **2008**, *46*, 2741–2753.
- (66) Kienzle, P. A.; O’Donovan, K. V.; Ankner, J. F.; Berk, N. F.; Majkrzak, C. F. <http://www.ncnr.nist.gov/refpak>, 2000–2006.
- (67) Azuah, R. T.; Kneller, L. R.; Qiu, Y.; Tregenna-Piggott, P. L. W.; Brown, C. M.; Copley, J. R. D.; Dimeo, R. M. *J. Res. Natl. Inst. Stand.* **2009**, *114*, 341–358.
- (68) Soles, C. L.; Douglas, J. F.; Wu, W. L.; Dimeo, R. M. *Macromolecules* **2003**, *36*, 373–379.
- (69) Soles, C. L.; Douglas, J. F.; Wu, W. L. *J. Polym. Sci., Part B* **2004**, *42*, 3218–3234.
- (70) Priestley, R. D.; Broadbelt, L. J.; Torkelson, J. M.; Fukao, K. *Phys. Rev. E* **2007**, *75*, 765–771.
- (71) Dalnoki-Veress, K.; Forrest, J. A.; Murray, C.; Gigault, C.; Dutcher, J. R. *Phys. Rev. E* **2001**, *63*, 031801.
- (72) Cicerone, M. T.; Zhong, Q.; Johnson, J.; Aamer, K. A.; Tyagi, M. *J. Phys. Chem. Lett.* **2011**, *2*, 1464–1468.
- (73) Fakhraei, Z.; Forrest, J. A. *Science* **2008**, *319*, 600–604.
- (74) Simmons, D. S.; Douglas, J. F. *Soft Matter* **2011**, *7*, 11010–11020.
- (75) Riggelman, R. A.; Douglas, J. F.; de Pablo, J. J. *Soft Matter* **2010**, *6*, 292–304.
- (76) Hall, R. W.; Wolynes, P. G. *J. Chem. Phys.* **1987**, *86*, 2943–2948.
- (77) van Zanten, J. H.; Rufener, K. P. *Phys. Rev. E* **2000**, *62*, 5389–5396.
- (78) Inoue, R.; Kanaya, T.; Nishida, K.; Tsukushi, I.; Shibata, K. *Phys. Rev. Lett.* **2005**, *95*, 056102.
- (79) Torres, J. M.; Stafford, C. M.; Vogt, B. D. *Polymer* **2010**, *51*, 4211–4217.
- (80) Forrest, J. A.; Dalnoki-Veress, K. *ACS Macro Lett.* **2014**, *3*, 310–314.
- (81) Squires, G. L. *Introduction to the Theory of Thermal Neutron Scattering*, 3rd ed.; Cambridge University Press: New York, 2012.
- (82) Soles, C. L.; Dimeo, R. M.; Neumann, D. A.; Kisliuk, A.; Sokolov, A. P.; Liu, J. W.; Yee, A. F. *Macromolecules* **2001**, *34*, 4082–4088.
- (83) Rotella, C.; Wubbenhorst, M.; Napolitano, S. *Soft Matter* **2011**, *7*, 5260–5266.
- (84) Glynos, E.; Frieberg, B.; Green, P. F. *Phys. Rev. Lett.* **2011**, *107*, 118303.
- (85) Stukalin, E. B.; Douglas, J. F.; Freed, K. F. *J. Chem. Phys.* **2010**, *132*, 084504.
- (86) Buchenau, U.; Zorn, R. *Europhys. Lett.* **1992**, *18*, 523–528.
- (87) Larini, L.; Ottochian, A.; De Michele, C.; Leporini, D. *Nat. Phys.* **2008**, *4*, 42–45.
- (88) Simmons, D. S.; Cicerone, M. T.; Zhong, Q.; Tyagi, M.; Douglas, J. F. *Soft Matter* **2012**, *8*, 11455–11461.
- (89) Simmons, D. S.; Cicerone, M. T.; Douglas, J. F. *Soft Matter* **2013**, *9*, 7892–7899.
- (90) Soles, C. L.; Douglas, J. F.; Wu, W. L.; Dimeo, R. M. *Phys. Rev. Lett.* **2002**, *88*, 037401.
- (91) Soles, C. L.; Douglas, J. F.; Wu, W. L.; Peng, H. G.; Gidley, D. W. *Macromolecules* **2004**, *37*, 2890–2900.
- (92) Huang, R.; Stafford, C. M.; Vogt, B. D. *J. Aerospace Eng.* **2007**, *20*, 38–44.
- (93) de Gennes, P. G. *Eur. Phys. J. E* **2000**, *2*, 201–203.